

Intra-Motion Compensation Using CSRS method in MRI

Y. M. Ro^{*,**} · J. H. Yi^{**} · Z. H. Cho^{**}

=Abstract=

In the conventional Fourier imaging method in MRI (Magnetic Resonance Imaging), intra-motion such as pulsatile flow makes zipper-like artifact along the phase encoding direction. On the other hand, line-integral projection reconstruction (LPR) method has advantages such as imaging of short T₂ object and reduction of the flow artifact by elimination of the flow-induced phase fluctuation. The LPR, however, necessarily requires time consuming filtering and back-projection processes, so that the reconstruction takes long time. To overcome the long reconstruction time of the LPR and to obtain the flow artifact reduction effect, we adopted phase corrected concentric square raster sampling (CSRS) method and improved its imaging performance. The CSRS is a fast reconstruction method which has the same properties with the LPR. In this paper, we proposed a new method of flow artifact reduction using the CSRS method. Through computer simulations and experiments, we verified that the proposed method can eliminate phase fluctuations, thereby reducing the flow artifact and remarkably shorten the reconstruction time which required long time in the LPR.

Key words : MRI, Intra-motion, Flow artifact, CSRS

INTRODUCTION

Since the magnetic resonance imaging (MRI) method was introduced, a lot of imaging techniques have been developed to satisfy various diagnostic purposes as well as to overcome various physical problems¹⁻⁶⁾. One of the problems in in-vivo human imaging is intra-motion of object such as, pulsatile blood flow, CSF flow, and abdominal motion. Such moving particles cause random phase shift in acquired data, so that the image is degraded with ghost and blur⁷⁾. In the conventional Fourier imaging, called KWE method, these artifacts appear in the direction of phase encoding due to longer time interval between RF excitations compared with velocity of particles.

The line-integral projection reconstruction (LPR) has a

useful property that is reducing the flow artifact caused by the flow. Because of the reconstruction algorithm of the LPR imaging is performed in real object domain, the phase term is eliminated by taking magnitude value while the KWE method is processed in spatial frequency domain, i. e., complex domain. The phase shift is spreaded over the whole image domain, in the LPR method, the image degradation due to the flow is reduced less than the KWE method⁸⁾. The LPR method, however, requires long reconstruction time because of its complex reconstruction scheme; i. e., filtering and filtered back-projection processes. Therefore, we adopted a fast reconstruction method named modified concentric square raster sampling scheme (CSRS), which is based on the Concentric Square Raster Sampling Scheme⁹⁾. Even though the data set of the CSRS method is

* Dept. of Computer Sciences, Taejon University 96-3 Yong Woon-don dong-gu, Taejon, Korea

** Dept. of Information & Communication Engineering, KAIST, 207-43 Cheongryani, Seooul, Korea

통신저자: Y. M. Ro, (130-012) 서울특별시 동대문구 청량리동 207-43, Tel. (02) 958-3352, Fax. (02) 965-4394

obtained by the similar way with the LPR method, reconstruction process of the CSRS method is performed in the frequency domain using the fast Fourier transform (FFT).

EFFECT OF FLOW IN MRI

The motion and flow effects are appeared by the two different ways in MR imaging; time-of-flight and phase shift in the NMR signal. The time-of-flight effect makes the NMR signal larger or smaller according to the circumstances (e. g., T_R , T_E , T_1 , T_2 and flow speed) without any geometrical distortion.

The flow-induced phase is induced by spins moved in the gradient field. The phase shift in NMR signal due to flow of velocity is described as

$$\phi(t) = r \int_0^t G(t') \cdot v(t') t dt, \quad (1)$$

is started from 90° RF excitation; i. e., the 90° RF pulse is applied at $t=0$. The spin density function $\rho(x, y)$ can be separated into stationary and flowing components;

$$\rho(x, y) = \rho_s(x, y) + \rho_v(x, y), \quad (2)$$

where, ρ_s and ρ_v are stationary and moving components, respectively. If one uses the y gradient as a readout gradient, fluctuation of the flow induced phase shift in the ty direction is negligible because the data sampling duration in ty direction is short enough, i. e., less than 20ms. Therefore, the phase shift due to the flow is dependent only on the tx, i. e., the phase encoding direction. By considering the flow-induced phase term, NMR signal is expressed as;

$$\begin{aligned} S(tx, ty) &= \int_{-\infty}^{\infty} \int_{-\infty}^{\infty} \rho_v(x, y) \exp[-i\gamma(xG_x tx + yG_y ty)] dx dy \\ &= S_v(tx, ty) \exp[i\phi_v(tx)], \end{aligned} \quad (3)$$

By taking a two-dimensional Fourier transform of Eq. (3), the flow affected NMR image can be obtained as

$$\rho_v(x, y) = \rho_v(x, y) * \Phi_v(x) \quad (4)$$

where is $\Phi_v(x)$ a Fourier transform of $\exp[i\phi_v(tx)]$ and * is

where $G(t)$ is the time-varying gradient field and $v(t)$ is the velocity vector of the flowing spin. In Eq. (1), the time convolution operator. As shown in Eq. (4), the resultant image can be considered as the flow artifact free image $\rho_v(x)$ convolved with $\Phi_v(x)$. If the $\phi_v(tx)$ is a random function, the $\Phi_v(x)$ also becomes random function and this is why the flow artifacts in Fourier NMR image appeared as discrete random noise along the coding direction.

CSRS ALGORITHM

The CSRS algorithm is based on the projection theorem⁹⁾: The image reconstruction is carried out in the frequency domain using the FFT⁸⁾. According to projection theory, NMR signals are Fourier transforms of the projections. To convert polar projection data to rectangular image data, interpolation processes are necessary. The interpolation process, however, causes error and requires long time. To reduce the error and processing time, a modified CSRS method was presented⁹⁾. To reduce the interpolation error in the modified CSRS method, the sampling rate is increased in 45° and 135° direction as shown in Fig. 1.

In the modified CSRS method, frequency domain sampling interval at a view angle θ_i is;

$$\Delta w(\theta_i) = \Delta w(0) \frac{1}{\max(|\cos\theta_i|, |\sin\theta_i|)} \quad (5)$$

where, $\Delta w(0)$ is a sampling interval when the $\theta = 0$,

$$\theta = \frac{\pi}{2}.$$

With a fixed number of sampling points N, the spatial domain sampling interval (ΔR) and span of the sampling (R) become

$$\Delta R(\theta_i) = \Delta R(0) \cdot \max(|\cos\theta_i|, |\sin\theta_i|), \quad (6)$$

$$R(\theta_i) = N\Delta R(0) \cdot \max(|\cos\theta_i|, |\sin\theta_i|), \quad (7)$$

The path of $R(\theta_i)$ is shown in Fig. 1.(b). To avoid the interpolation error, the vertical (or horizontal) distance between neighboring sample points Δw_y (or Δw_x) should be kept equality by increasing the number of views towards

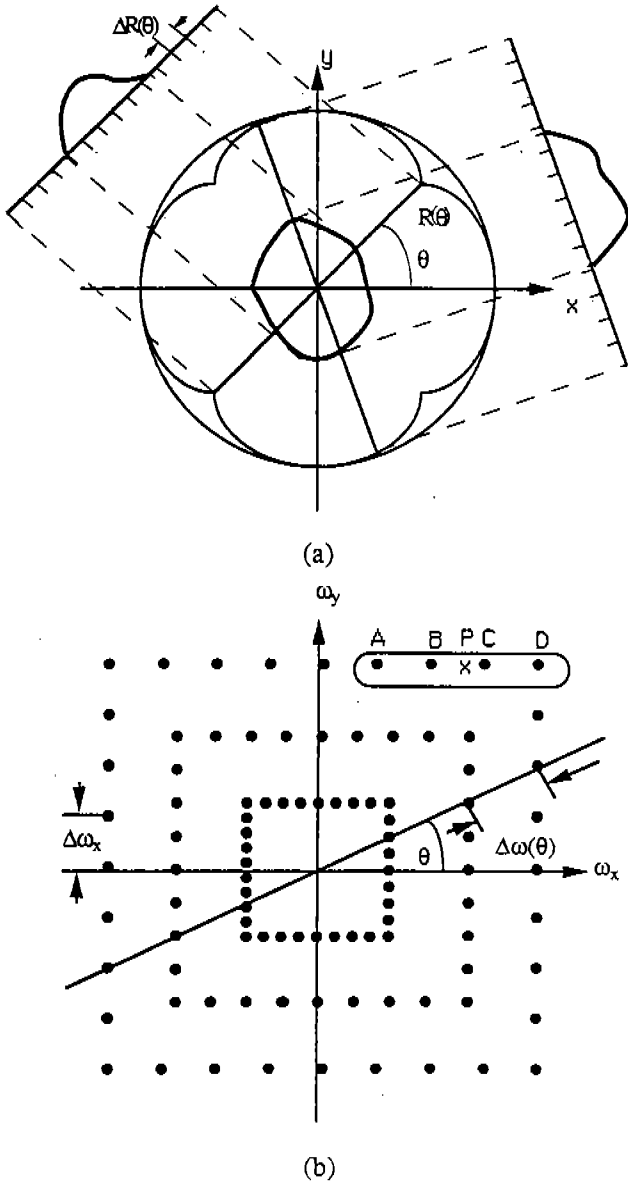


Fig. 1. Sampling scheme in frequency domain. Sampling interval is changed according to the projection angle θ . Equal $\Delta\omega_x$ (or $\Delta\omega_y$) is resultant interval in the direction of horizontal (or vertical).

45° and 135° direction. The view angle, then, will be expressed as,

$$\begin{aligned}
 \theta_i &= \tan^{-1}\left(\frac{i-1}{N/4}\right), \quad \text{for } i = 1, 2, \dots, \frac{N}{4} + 1 \\
 \frac{\pi}{2} - \theta_{\frac{N}{2} + 2 - i} & \quad \text{for } i = \frac{N}{4} + 2, \dots, \frac{N}{2}, \\
 \frac{\pi}{2} + \theta_{i - \frac{N}{2}} & \quad \text{for } i = \frac{N}{2} + 1, \dots, N
 \end{aligned} \tag{8}$$

Using this technique, the interpolation error could be kept nearly the same for all the frequency space, thereby improving the image quality. Another approach to reduce the interpolation error is the high order interpolation. For this purpose four-point Lagrange interpolation was used. The interpolation is performed along the vertical and horizontal line of resulting image. Because of the raster sampling provides higher sampling rate in the central region of the frequency data, exact interpolation is obtained for low frequency components of the image.

FLOW ARTIFACTS IN CSRS METHOD

In contrast to the Fourier imaging in which the phase information is related to the spatial position by Fourier transform relationship, the CSRS method uses magnitude of the projection. Therefore, the flow-related phase errors will be appeared with different way as in the LPR method.

The NMR signal of CSRS method is expressed as

$$S(\theta;t) = \int_{-\infty}^{\infty} \int_{-\infty}^{\infty} \rho(x', y') \exp(-iy'Gx't) dx' dy', \tag{9}$$

where θ is the projection angle, $\rho(x', y')$ is the spin density function of a selected slice, and $x' (=x \cos\theta + y \sin)$, $y' (= -x \sin\theta + y \cos\theta)$ are the rotated coordinate variables. One-dimensional Fourier transform of $S(\theta;t)$ is complex value and its magnitude can be regarded as the projection data of the object. Then the projection data of projection angle θ is

$$\begin{aligned}
 p(\theta;x) &= |\mathcal{F}[S(\theta;t)]| \\
 &= \left| \int_{-\infty}^{\infty} \rho(x', y') dy' \right|
 \end{aligned} \tag{10}$$

where \mathcal{F} denotes Fourier transform operation.

If flow induced phase shift is $\phi_v(\theta)$, the NMR signal becomes

$$S(\theta;t) = S(\theta;t) \exp[i\phi_v(\theta)]. \tag{11}$$

If one use real part in Eq. (11) as the projection data, the effect of the phase shift due to the flowing spins can be reduced in the reconstruction, i. e., flow artifacts can be red-

used. The projection data can be written as

$$\begin{aligned}
 p(\theta; x) &= |\mathcal{F}[S(\theta; t) \exp[i\phi_v(\theta)]]| \\
 &= |\exp[i\phi_v(\theta)] \mathcal{F}[S(\theta; t)]| \\
 &= |\mathcal{F}[S(\theta; t)]| \\
 &= p(\theta; x)
 \end{aligned}
 \tag{12}$$

However, this is only for the case where all the spins have constant phase shift. When there are stationary component and flowing component together in the object, e. g., $\rho(x', y) = \rho_v(x', y) + \rho_s(x', y)$, then the NMR signal will become

$$\begin{aligned}
 S(\theta; x) &= \int \int_{-\infty}^{\infty} [\rho_s(x', y) + \rho_v(x', y) \exp[i\phi_v(\theta)]] \exp(-i \\
 &\gamma G x' t) dx' dy',
 \end{aligned}
 \tag{13}$$

and corresponding projection is

$$\rho(\theta; x) = \left| \int \int_{-\infty}^{\infty} [\rho_s(x', y) + \rho_v(x', y) \exp[i\phi_v(\theta)]] dy' \right|.
 \tag{14}$$

Equation(14) is not the correct projection data since the equation includes phase error term. The phase interference produces star-like streak artifacts in the modified CSRS imaging because this method corrects the phase error in the radial direction. However, the flow artifact will not appear along one particular direction since it spreaded over 2π direction.

Advantage of the CSRS by comparing with LPR is fast reconstruction. The LPR is based on filter back-projection. The back-projection process requires considerably long calculation time. For $M \times M$ image with N sample per line, the number of multiplies is $M^2 N$. On the contrary, the CSRS is a fast reconstruction algorithm because it uses the FFT. Hence, the calculation is M^2 . By using the CSRS algorithm, the calculation amount can be reduced to M^2 order from M^3 order.

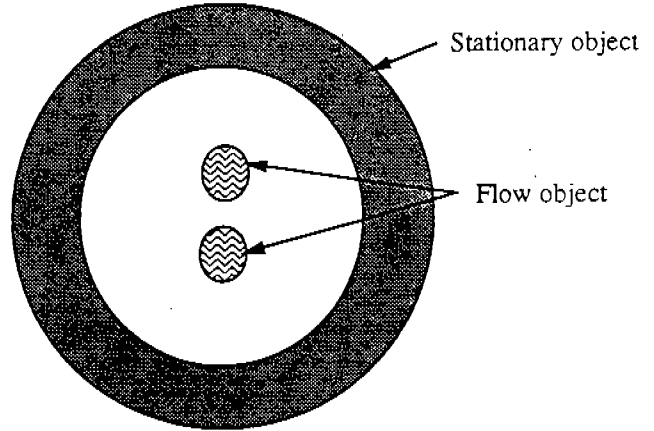


Fig. 2. A simulation phantom. Outside ring filled with stationary spins and inner two circles are filled with flowing with random phase errors.

SIMULATION AND EXPERIMENTAL RESULTS

Simulations and experiments were performed for the flow phantom shown in Fig. 2. The simulation results for the flow phantom are shown in Fig. 3(a)-(c) for KWE, LPR, and CSRS imaging methods, respectively. The cut views represent reduced flow artifacts in the PPR as well as CSRS, which manifest that the LPR and CSRS methods have flow artifact reduction effect while the artifacts are severe in the phase-encoding direction for the KWE imaging.

Experiments were performed using 2.0 T whole body MRI system. To prevent the chemical shift artifact in LPR and CSRS due to different resonance frequency of water and fat, the view angle tilting method is added. The gradient magnitude for each coding steps are shown in Fig. 4(a) and (b). We maintained the imaging parameters over the whole experiments to compare their effect exactly as shown in Table 1.

The flow phantom imaging is shown in the Fig. 5(a)-(c) for KWE, LPR, and CSRS, respectively. In the KWE

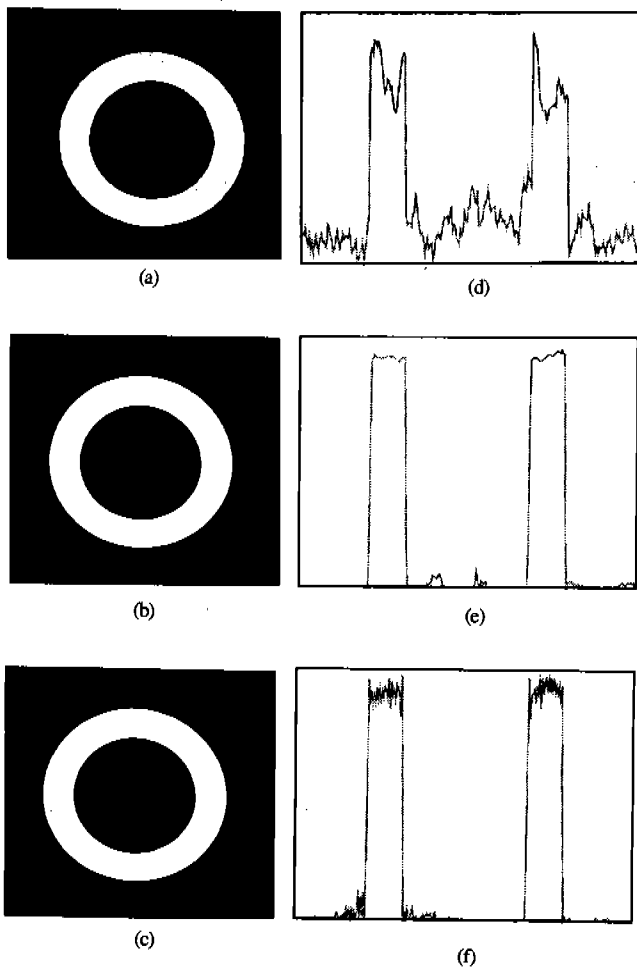


Fig. 3. Simulations results of the flow phantom. Simulation are performed for KWE, LPR, and CSRS methods. The flow artifacts in KWE method appear in the phase encoding direction as shown in (a) and (b). In LPR and CSRS method, the flow artifacts are reduced as shown in (b) and (c) respectively. The cut profiles of the images are shown in (e) and (f).

imaging, severe flow artifacts are appeared along the phase encoding direction as shown in Fig. 5(a), while the artifacts are reduced in the LPR and CSRS as shown in Fig. 5 (b) and (c). The Reconstruction times of CSRS and LPR method in VAX-780 system take 1 minute 56 second and 30 minute, respectively.

CONCLUSIONS

Through the simulations and the experiments, we have proved the flow artifact reduction effect of the LPR and

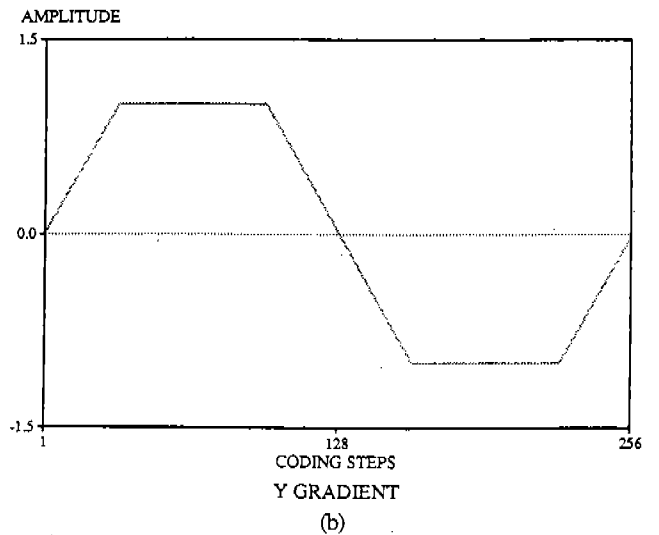
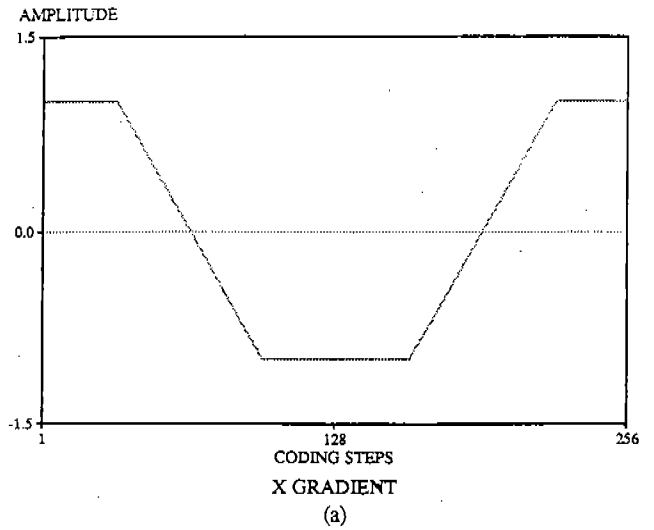


Fig. 4. Gradient magnitude for CSRS method. These make equal Δw_x (or Δw_y) in horizontal (or vertical) direction.

Table 1.

Repetition time	1000ms
Echo time	30ms
FOV	256mm
Slice thickness	5mm
Number of coding steps	256

CSRS methods by adding phase correction technique. The proposed CSRS method with phase correction spreads the flow-induced error to 2π direction so that the new method

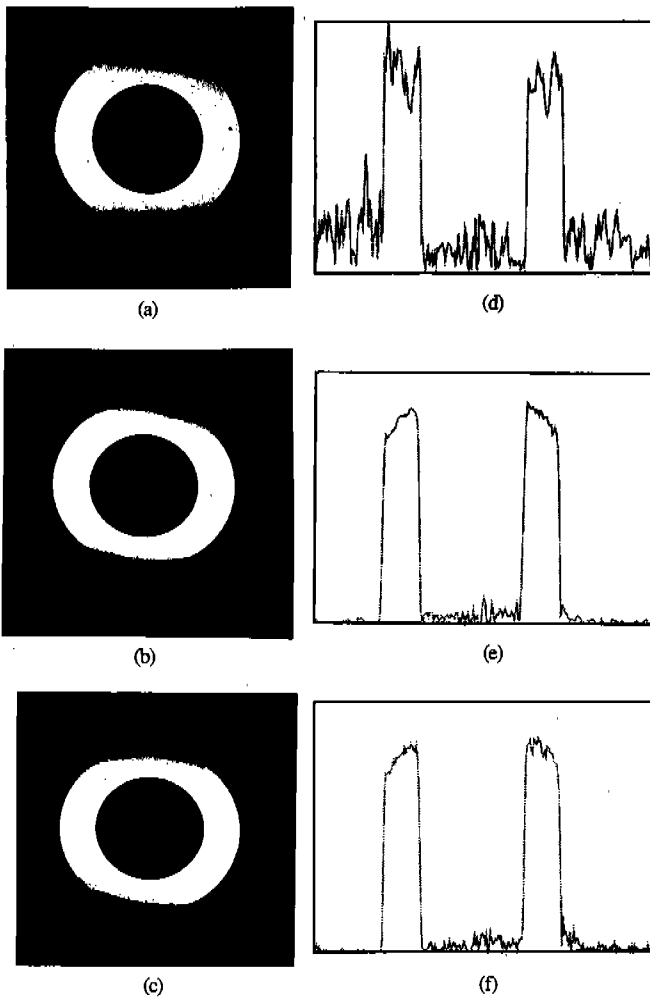


Fig. 5. Experimental results of a flow phantom. The phantom is same as that used in the simulations. Experiments are performed for KWE, LPR, and CSRS: The results are shown in (a),(b), and (c), respectively. As shown in it's cut view, flow artifacts appear only in KWE method while the artifacts are remarkably reduced in LPR and CSRS method.

improves the image quality, which is similar to LPR imaging. Unique advantage of proposed method is fast reconstruction; reconstruction speed of the proposed method is as fast as fifteen times than that of LPR.

REFERENCES

1. A. Kumar, D. Welte, and R. R. Ernst, "NMR Fourier Zeugmatography", J. Magn. Reson. 1975;18;69
2. Z. H. Cho, H. S. Kim, H. B. Song, and J. Cimring, "Fourier transform nuclear magnetic resonance tomographic imaging", Proc. IEEE 1982;70;1152
3. L. A. Shepp, and B. F. Logan, "The Fourier reconstruction of a head section", IEEE Trans. NS 1974;21;21
4. D. Shaw, "Fourier transform NMR spectroscopy", Elsevier Scientific Publishing Company, Amsterdam-Oxford-New York 1976.
5. D. E. Dudgeon, R. M. Mersereau, "Multidimensional Digital Signal Processing", Prentice-Hall, Inc. 1984;369.
6. R. M. Mersereau and A. V. Oppenheim, "Digital reconstruction of multidimensional signals from their projections", IEEE Proc. 1974;62;1319.
7. Y. M. Ro, and Z. H. Cho, "A Novel Flow-Suppression Technique Using Tailored RF Pulses", Magn. Reson. in Med. 1993;29;660-666.
8. K. J. Jung and Z. H. Cho, "Reduction of Flow Artifact in NMR Diffusion Imaging Using View-Angle Tilted Line-Integral Projection Reconstruction", Magn. Reson. Med. 1991;19;349-360.
9. Z. H. Cho, O. Nalcioglu, J. C. Jung, and H. B. Song, "Direct Fourier Reconstruction Technique in NMR tomography", Selected Topics in Imaging Science, Eds. O. Nalcioglu and Z. H. Cho, Springer-Verlag, Berlin, 1984; 40-60.